A computational view of the brain plasticity at rest

Invernizzi, Azzurra

DOI:
10.33612/diss.183130118

Chapter 5

rTMS treatment of visual hallucinations using a connectivity-based targeting method - A case-study

A condensed version of this chapter was published as a letter to the editor as:

Invernizzi A
Halbertsma HM
van Ackooij M
Bais L
Boertien J
Renken RJ*
Cornelissen FW*
van Laar T* (2019)

*These authors contributed equally to this work

Brain Stimulation 12 (2019) 1622-1624

ABSTRACT

Visual hallucinations (VH) are difficult to treat because pharmacological interventions are only partially effective and associated with many adverse effects. One of the alternative non-pharmacological treatments for VH is repetitive transcranial magnetic stimulation (rTMS). However, identifying optimal stimulation sites for rTMS is challenging.

To determine whether a connectivity-based targeting approach based on resting state (rs) fMRI data can be used to identify regions that may serve as effective rTMS targets. We acquired rs-fMRI scans pre-rTMS and post-rTMS in a single patient with retinitis pigmentosa (near blindness), Parkinson's disease (PD) and had therapy-resistant VH. Rs-fMRI data were analyzed using fast Eigenvector Centrality Mapping (ECM). A target area was selected based on high ECM values and relative accessibility for rTMS. Subsequently, the patient was stimulated with 1 Hz rTMS during 5 days, followed by 30 Hz theta-burst stimulation during another 5 days. Distributions of surrogate and bootstrap data were used to statistically evaluate the effect of rTMS. The bilateral supplementary motor areas (SMA) were selected as rTMS target areas. When pre-rTMS were compared to post-rTMS, different ECM values were found in the SMA, precuneus, occipital pole and hippocampus. Clinical evaluation and follow-up showed that the intensity and frequency of the VH were decreased after rTMS. Our connectivity-based targeting approach applied to rs-fMRI data seems to be successful in identifying an optimal target area for rTMS on a single subject basis. Our results show changes in the connectivity pattern, both in the target area and associated hubs involved in VH pathogenesis.

Highlights:

- Using rs-fMRI, we successfully identified target areas for rTMS treatment of VH.
- ECM revealed hubs that potentially underlie the pathogenesis of VH.
- rTMS stimulation induces effects that propagate beyond the immediate target area.

5.1 INTRODUCTION

Visual hallucinations (VH) are conscious visual perceptions that occur in the absence of an external stimulus. VHs are neuro-ophthalmological dysfunctions that are very disabling and are based on various pathologies, including eye diseases (Manford 1998) and neurodegenerative disorders (Waters et al. 2014). VHs are especially prevalent in patients with Parkinson's disease (PD): they affect 40% of PD patients. VHs are difficult to treat, and pharmacological treatment possibilities are limited, also in PD. Many patients have therapy-resistant VH.

Repetitive Transcranial Magnetic Stimulation (rTMS) has been suggested as a potential alternative treatment to reduce the frequency and intensity of VH (Jolfaei, Naji, and Esfehani 2016; Fregni and Pascual-Leone 2007; Dayan et al. 2013). rTMS is a non-invasive brain stimulation technique that uses a rapidly changing magnetic field to induce either inhibitory or excitatory currents (Hallett 2007). One of the issues limiting a more widespread application of rTMS for treatment of VH is determining the most optimal treatment stimulation site (Fox et al. 2014; Sale et al. 2015). Usually, the same cortical stimulation site is used for all patients with a particular diagnosis. However, this does not account for possible inter-subject variability, both in functional neuroarchitecture and clinical symptoms (Hallett 2007). If we determined the optimal target site for rTMS in individual patients with different underlying pathologies and a range of VH experiences, this could improve the efficacy of rTMS as therapeutic treatment.

Several studies have used functional connectivity, based on rs-fMRI or task-based fMRI data (Jolfaei, Naji, and Esfehani 2016; Hoffman et al. 2007; Singh et al., n.d.), to guide and improve rTMS treatment of hallucinations. For instance, rs-fMRI was used to guide rTMS in a small group of patients with schizophrenia suffering from severe auditory hallucinations, but this did not result in a significant improvement (Hoffman et al. 2007). Two case studies on VH used fMRI to identify the occipito-temporal sulcus and the visual cortex as target regions for rTMS treatment (Jolfaei, Naji, and Esfehani 2016; Meppelink et al. 2010; Jardri et al. 2009). However, the relevance of interaction between brain areas was not taken into account, and post-treatment quantification with fMRI was lacking.

So far, no data have been published on the implementation of fast Eigenvector Centrality Mapping (Wink et al. 2012) (fast ECM) being used to optimize rTMS target site localization in patients with therapy-resistant VH.

In the current study, we used a novel connectivity-based targeting approach, based on rs-fMRI data, to identify regions of high-connectivity ("hubs") within functional brain

networks. We used these regions as target sites for rTMS treatment in a single case study. The approach reduced therapy-resistant VH in this subject. Our results also show changes in the connectivity pattern, both in the target area and associated hubs involved in VH indicating our approach can be used to obtain objective evidence for the efficacy of rTMS treatment for VHs.

5.2 METHODS

The fast ECM (Wink et al. 2012) method provides a whole-brain spatial characterization of the functional networks that are active over time, using the concept of node centrality. This method attributes an eigenvector value to each region of interest (ROI). This enables identification of influential hubs within a certain network that can subsequently be used as a target for rTMS treatment.

5.2.1 Case Study

The case study involved a 67-year-old female patient who was diagnosed with Parkinson's disease (PD) at the age of 62. Her hallucinations started two years after she had been diagnosed with PD, at the time of her first L-dopa treatment. In addition, she was diagnosed with retinitis pigmentosa (RP) 30 years previously, which was gradually progressive and resulted in Charles Bonnet syndrome (Hartong, Berson, and Dryja 2006). She had severely reduced vision in the right eye and only light perception in her left eye.

The visual hallucinations were mostly present during the daytime, when she had her eyes open, and consisted of two categories: 1) dynamic lifelike scenarios (VH-ds), such as scenes with people (women and children) and moving objects likes shovels, roads and comics figures, and 2) visual phenomena (VH-vp) like lights, sensations of waves and colors and the feeling of driving backwards in a car. All conventional pharmacological treatments in adequate doses, including clozapine, rivastigmine, quetiapine and olanzapine, failed to improve her VH, and were discontinued. Additional genetic testing, including a Parkinson gene panel and screening for mitochondrial mutations, did not reveal any abnormality. Cognitive screening at the time of this experimental procedure showed that the patient had mild cognitive problems, but she did not meet the criteria for PD-related dementia (MOCA 19/22; note that not all items could be tested due to her visual limitation).

The participant provided written informed consent. This study followed the tenets of the Declaration of Helsinki.

5.2.2 Experimental procedure

An outline of the experimental design can be found in Figure 1. A baseline fMRI scan was performed to acquire a first impression of potential functional neural networks involved in the VH of our subject and to see if the planned scanning procedures were tolerated and acceptable for the patient (Figure 1, Panel A). An important observation was that the patient could diminish her VH experiences by closing both her eyes. Therefore, two conditions were tested: daytime (bright screen and eyes open) and nighttime (darkened room and closed eyes). The final fMRI protocol (Figure 1, Panel B) was selected based on the outcome and evaluation of this baseline measurement (Figure 1, Panel A). Following the fMRI data acquisition, the patient was treated with rTMS (Figure 1, Panel B) applied to target areas that were determined as explained below (See Results section). The clinical assessment consisted of brief daily interviews with the patient to obtain qualitative data on the content and intensity of her VH during the first two weeks (Figure 1, Panel B). After 15 months, the rTMS treatment with theta burst stimulation was repeated (Figure 1, Panel C) using the same target areas.

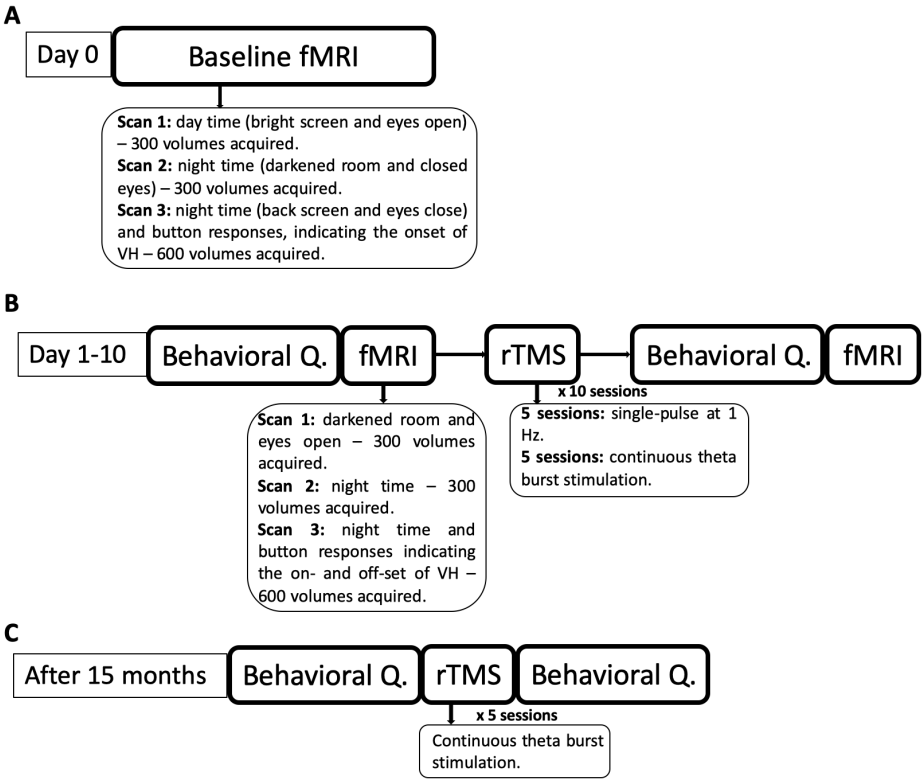

Figure 1. Flowchart of the study design. A: Baseline session. **B:** First rTMS treatment period. **C:** Second rTMS treatment period.

5.2.3 Assessment of visual hallucinations

The VH were scored daily during the rTMS treatment, using a diary with 2 categories of VH: dynamic scenes with people and objects (VH-ds) and visual phenomena (VH-vp). Both categories were rated by a Numeric Rating Scale (NRS) from 0 (not present) to 10 (very disturbing). The overall score consisted of the mean NRS scores of both VH categories.

5.2.4 MRI and fMRI data acquisition

Data acquisition was performed on a Siemens Prisma (Siemens; Erlangen, Germany) 3T scanner with a standard 64-channel head coil. Functional MR images were recorded using a single-shot gradient echo planar imaging (EPI); T2*-weighted. Slices were acquired in ascending order with an axial orientation and a voxel size of 2.4 mm isotropic and no slice gap; the repetition time (TR) was set to 0.73 s, and the echo time (TE) to 39 ms. For each EPI sequence, an additional intra-run motion correction MOCO sequence was produced by the scanner, using the first volume as reference. Additionally, a 3D high-resolution anatomical scan (MPRAGE) was acquired using T1-weighted gradient echo sequence. Slices were acquired with matrix size of 240 x 256 in axial orientation and voxel size of 1 mm isotropic; the TR was set to 2.3 s, and the TE to 2.98 ms.

5.2.5 Data analysis

Image preprocessing, functional network analysis and statistical analyses were performed using SPM12 (Wellcome Department of Imaging Neuroscience, London, UK), fastECM toolbox (Wink et al. 2012) and customized scripts, implemented in Matlab 2014b (Mathworks).

5.2.5.1 Image preprocessing

The structural MR image (T1 weighted) was co-registered and normalized to the Montreal Neurological Institute (MNI) template and segmented in order to obtain white matter (WM), grey matter (GM) and cerebrospinal fluid (CSF) probability maps in MNI space.

FMRI data were spatially realigned, co-registered to the MNI-152 EPI template, and subsequently normalized using the deformation field obtained in the segmentation step. All normalized data was resampled to a 3 mm isotropic voxel resolution. Additionally, spatial smoothing was applied (8 mm) to fMRI. No global signal regression was applied.

5.2.5.2 Fast Eigenvector Centrality Mapping

Average time series were extracted and fast ECM was performed on 111 ROIs (96 cortical and 15 subcortical brain areas) based on a customized version of the Harvard-Oxford Atlas, during which the corresponding ROIs were labeled uniquely for the left and right hemisphere separately.

The ECM method builds on the concept of node centrality, which spatially characterizes functional networks active over time and attributes a voxel-wise centrality value to each ROI. Such a value is strictly dependent on the sum of centrality properties of the direct neighbor nodes within a network. In the fast ECM toolbox, EC is estimated from the adjacency matrix, which contains the pairwise correlation between the ROIs. To obtain real-valued EC value, we added +1 to the values in the adjacency matrix (Wink et al. 2012). Several ECM values can be attributed to a given node, but only the eigenvector with the highest eigenvalue will be assigned to it. Based on these values influential hubs could then be identified. To define the viable target areas, only those with the 10% highest ECM coefficients were considered as potential treatment areas.

5.2.5.4 Pre-whitening and statistical analysis

To facilitate statistical inference, data were "pre-whitened" by removing the estimated autocorrelation structure in a two-step GLM procedure (Monti 2011; Bright and Murphy 2015). In the first step, the raw data were filtered against the 6 motion parameters (3 translations and 3 rotations). Using the resulting residuals, the autocorrelation structures present in the data were estimated using an Auto-Regressive model of order 1 (AR(1)) and then removed from the raw data. Next, the realignment parameters, white matter (WM) and cerebrospinal fluid (CSF) signals were removed as confounders on the whitened data.

To obtain a proxy distribution for the null hypothesis, surrogate BOLD time series were generated 1000 times using the iterative amplitude adjusted Fourier transform method (iAAFT) (Räth and Monetti 2009; Schreiber and Schmitz 1996). In this way, correlations between ROIs were removed. Note that the null distribution of the ECM was not centered around zero, as ECM values were positive real-valued.

To define the confidence intervals of each ECM value estimated per ROI, a bootstrap technique (across time-point) was used in parallel to resample the filtered fMRI data 3000 times.

For each distribution obtained using the bootstrap and surrogate data, the median and the interquartile ranges (IQR) were computed. When comparing against the null distribution, we defined a result as significant when the median of the bootstrap results falls outside the 95% confidence interval of the null distribution. Furthermore, when comparing conditions, we considered a shift to be meaningful when the IQ ranges (obtained using bootstrap) do not overlap.

To support visualization, a Gaussian distribution was fitted to each distribution (Figure 4).

5.2.6 rTMS target region localization

Based on the highest ECM value found across the baseline and pre-treatment scans, and taking into consideration whether a particular cortical area was accessible for rTMS, an optimal target site for rTMS treatment was selected. Using the Harvard-Oxford atlas parcellation and the deformation field derived in the segmentation, the bilateral target areas were defined based on the anatomical scan of the subject in native space. During the treatment, the target site was localized using a frameless stereotaxy neuronavigation system (BrainVoyager TMS neuronavigation).

5.2.7 rTMS stimulation protocol

Two stimulation protocols were used. During the first five consecutive treatment days, 1 Hz rTMS was given at 90% of the resting motor threshold. Both hemispheres were stimulated for 20 minutes. After two weekend days without rTMS treatment, the patient received another five consecutive days of rTMS treatment with continuous theta burst stimulation (cTBS) at 30 Hz, for 80 sec per hemisphere. During both stimulation protocols, target areas were stimulated with 1200 pulses per session, with a total of 6000 pulses per hemisphere.

5.3 RESULTS

5.3.1 Identification of network hubs

We identified several hubs as being in the top 10% of hubs with highest ECM values (influential hubs; Table 1 and Figure 2). Specifically, the bilateral SMAs and the precuneus (PCN) were consistently amongst the most influential hubs during all the pre-treatment scanning sessions. Due to their cortical surface position, which makes them easily accessible for rTMS, the bilateral SMAs were selected as the optimal stimulation area for rTMS treatment. We checked the consistency of the baseline results using the pre-treatment scans. Similar functional connectivity patterns, involving bilateral SMAs, were found across baseline and pre-treatment scans, thus assuring consistency in the baseline results (Figure 2, panels A, B, C compared to panel D). This confirmed our selection of the SMA as a target area, based on the functional network.

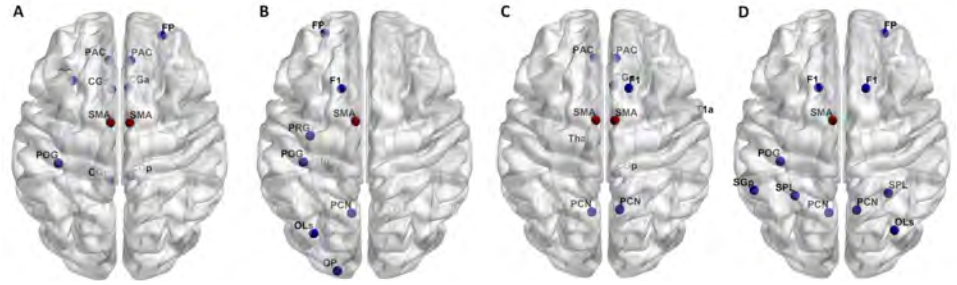

Figure 2. Functional connectivity network hubs. The 10% highest centrality values have been plotted for the baseline scans. During different conditions – bright screen and eyes open (A), dark screen and eyes closed (B and C) – SMA was associated with increased ECM values and visual experiences of the subject.

Table 1. ECM values during baseline and pre-rTMS scans.

ROIs	Scan 1	Scan 2	Scan 3	Scan 1
SMA Left	0.1071	0.1088	0.1058	0.1061
SMA Right	0.1073	–	0.1050	–
Cingulate Anterior Right	0.1062	–	0.1043	–
Cingulate Posterior Right	0.1067	–	0.1051	–
Paracingulate Left	0.1057	–	0.1016	–
Postcentral Gyrus Left	0.1066	0.1111	–	0.1066
Precuneus Left	–	0.1099	0.1016	0.1100

Only the 10% highest ROIs present in at least two over three scans are shown.

5.3.2 Functional centrality changes post rTMS

To monitor the effect of the treatment, we calculated the functional connectivity (FC) between the SMA and a collection of well-connected cortical hubs, known as the rich club (Sporns, Honey, and Kötter 2007; van den Heuvel and Sporns 2011). We compared the FC correlation coefficient between pre-treatment and post-treatment conditions and observed a distinct change in the connectivity pattern of the SMA. A selective increase of FC between bilateral SMAs and the hippocampal formation was noticed in post-rTMS scan (Figure 3). At the same time, a decrease in FC was observed involving bilateral SMAs and putamen (Figure 3).

5.3.3 Quantification of ECM changes between pre- and post-rTMS

To quantify the significance of the overall changes observed in FC, bootstrap and surrogate methods were both applied to the ECM value of each node. For pre-rTMS and post-rTMS, this procedure was applied to all experimental conditions, including eyes-open and eyes-closed. Table 2 and Figure 4 show the bootstrap and surrogate distribution of centrality for four regions: SMA, PCN, hippocampal formation and occipital pole.

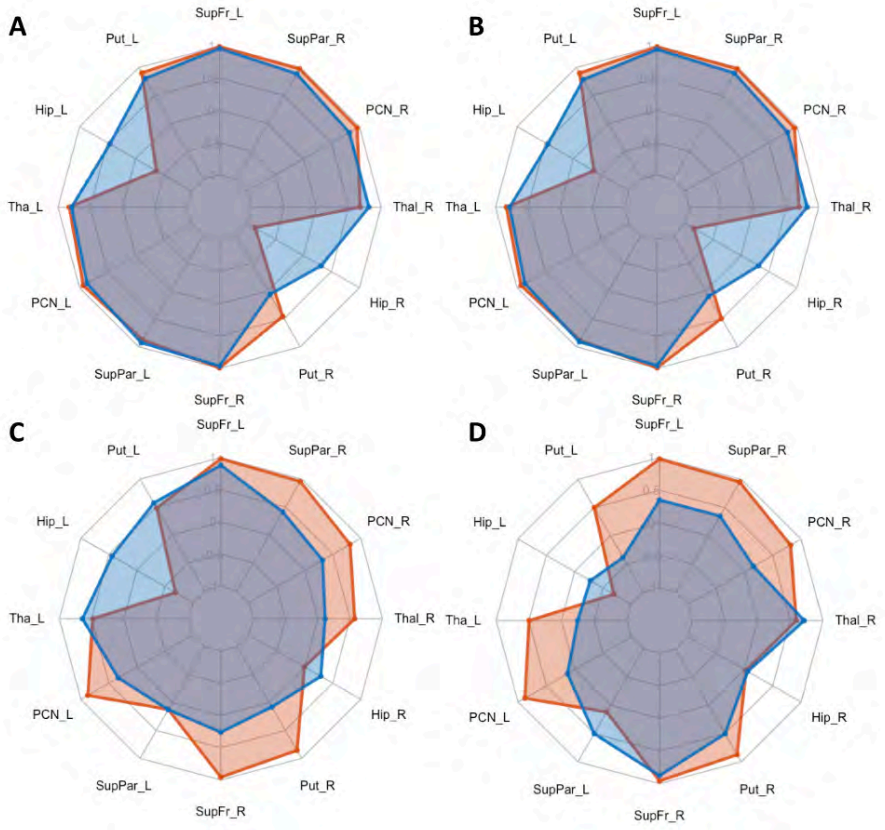

Figure 3. Connectivity fingerprints of SMA compared to the rich club areas. During eyes-closed fMRI, left and right SMA (**A** and **B**) show increased functional coupling in the hippocampal areas post-rTMS (blue) compared to the pre-rTMS (orange) session. During eyes-open fMRI, left SMA (**C**) shows increased FC with bilateral hippocampus post-rTMS. Right SMA (**D**) shows an increased FC only on the left hippocampal area and a stable FC with the right hippocampus.

Eigenvector values of the SMA – our target region for the rTMS treatment – showed a consistent and significant shift between the experimental conditions, including eyes-open and closed, for pre-rTMS and post-rTMS (Figure 4, Panel A; Table 2). The ECM values and bootstrapping distributions did not overlap pre-treatment and differed between conditions (Table 2). However, the ECM values for both conditions, and the bootstrap distributions for the eyes-open condition, did not differ significantly, showing an overlap with the null distribution.

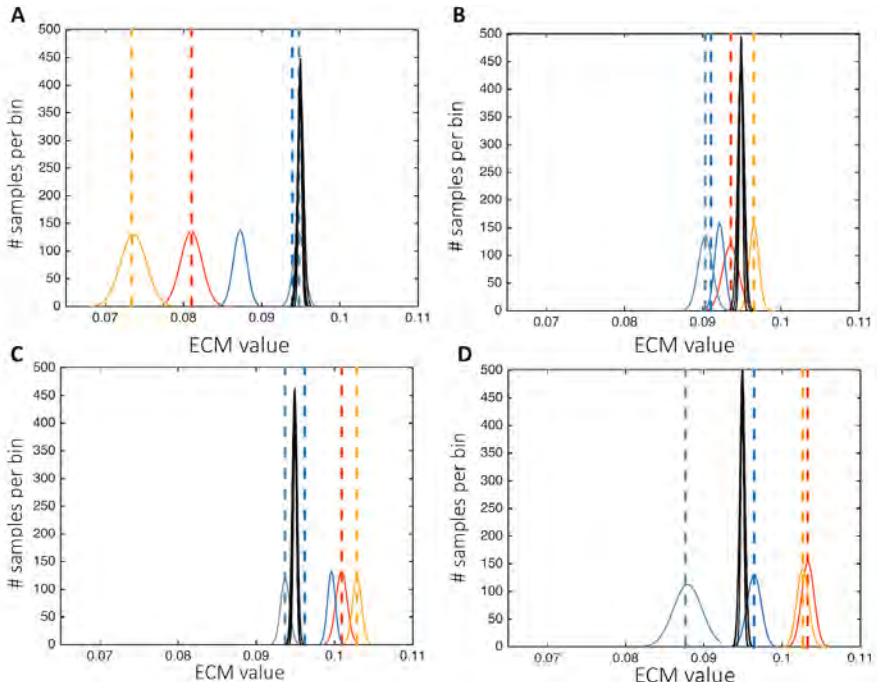

Figure 4. ECM values across conditions and areas. Eigenvector values for open and closed eyes pre-rTMS (light orange and orange dashed line) and post-rTMS (light blue and blue dashed line), bootstrapped distributions (solid line) and surrogates distributions (black lines) are shown for bilateral SMA (**A**), PCN (**B**), hippocampus (**C**) and occipital pole (**D**).

ECM values and overlapping bootstrap distributions in PCN, used as a control area in the given subject, did not show any difference between experimental conditions for pre-treatment and post-treatment (Figure 4, Panel B; Table 2). However, ECM values post-rTMS are similar in both conditions (eyes open and eyes closed).

Additionally, we statistically investigated the ECM value of the hippocampal formation due to the changes observed in FC analysis. We noticed a shift between experimental conditions for pre- rTMS and post-rTMS (Figure 4, Panel C; Table 2). Pre-treatment, ECM values differed between conditions. Post-treatment, only the median of the bootstrap distribution for the eyes-open condition did not deviate significantly from the null distribution (Table 2). A similar statistical outcome was observed in the SMA region.

Due to the near-total blindness of our patient, we determined whether the visual cortex, in particular the occipital pole, was influenced by the rTMS treatment. ECM values showed a consistent shift between pre-rTMS and post-rTMS (Figure 4, Panel

D; Table 2). Pre-rTMS, a similarity was observed between conditions: the distributions overlapped substantially. Post-rTMS, ECM values and bootstrap distributions were different between conditions. For the eyes-closed condition (resting state data), the ECM value was shifted towards the null distribution and no longer deviated significantly from it. In contrast, for the eyes open condition the ECM value shifted strongly towards the opposite side of the null distribution and still deviated significantly.

Table 2. **Bootstrap and Surrogates.**

		Bootstrap				Surrogates			
		RS		*Task*		*RS*		*Task*	
		median	*IQR*	*median*	*IQR*	*median*	*IQR*	*median*	*IQR*
SMA	pre - rTMS	0.0818	0.0047	0.0732	0.0054	0.0950	0.0013	0.0949	< 0.00
	post -rTMS	0.0868	0.0030	0.0946	0.0024	0.0949	0.0011	0.0949	< 0.00
PCN	pre - rTMS	0.0935	0.0024	0.0968	0.0018	0.0949	0.0012	0.0949	< 0.00
	post -rTMS	0.0922	0.0016	0.0905	0.0017	0.0950	0.0011	0.0949	< 0.00
Hip	pre - rTMS	0.1007	0.0031	0.1027	0.0024	0.0949	0.0016	0.0949	< 0.00
	post -rTMS	0.0995	0.0025	0.0937	0.0031	0.0950	0.0013	0.0950	< 0.00
OP	pre - rTMS	0.1033	0.0030	0.1029	0.0027	0.0950	0.0014	0.0950	< 0.00
	post -rTMS	0.0961	0.0030	0.0872	0.0051	0.0949	0.0014	0.0949	< 0.00

The median and interquartile range (IQR) for resting state and fMRI data are shown.

5.3.4 ECM changes and the effect on visual hallucinations

Clinical follow-up showed that the intensity and frequency of the VH decreased considerably, lasting for 6 months following the rTMS treatment. The observed ECM changes were accompanied by an overall improvement of 44% of the VH scores. The VH intensity at baseline started with a mean NRS of 8 (VH-ds 8 and VH-vp 8), which improved to a mean NRS score of 4.5 points at the end of the treatment (NRS VH-ds 3 and NRS VH-vp of 6 points). The patient noticed the improvement after the first treatment session with 1 Hz stimulation, and improvement continued during the course of the theta burst stimulation. Some repetitive phenomena were observed, existing of a short-lasting worsening of the VH (both types) during the stimulation, which was followed by a clear improvement thereafter. The improvement disappeared during the first days of the treatment, but eventually persisted. Importantly, the overall improvement was mainly related to the diminishing VH-ds. Finally, for the first time in 2 years, the patient reported some hours without any VH.

5.4 DISCUSSION

Our main finding is that ECM applied to resting state fMRI (rs-fMRI) based data can be used to identify a target area for successful rTMS treatment. Moreover, we showed that

the same ECM approach can be used to monitor the effectiveness of rTMS treatment. We used this approach in a case study of a patient with PD and RP who suffered from severe drug-resistant VH. Her RP has been progressive for many years, resulting in Charles Bonnet syndrome. However, in her case there appeared to be an additional influence due to her PD in combination with the L-dopa intake, although her cognitive performance did not indicate PD related dementia.

Using fECM, we identified the SMA as an influential hub that is strongly associated with regions known to be involved in auditory (Lima, Krishnan, and Scott 2016) and visual mental imagery (Labriffe et al. 2017). Moreover, post-rTMS we also observed significant changes in the SMA, the hippocampus and the occipital pole. This effect was absent in the PCN, which served as our control area. Subsequent to rTMS treatment we observed increased connectivity between the hippocampal formation and the "rich-club" network. Interestingly, this change correlated with the decrease in VH severity following the rTMS treatment. Long-term follow-up at the outpatient clinic showed a persistent positive effect after the rTMS treatment for up to 6 months, although showing a gradual loss in effect from 3 months onwards. Overall, our results support the use of individually customized rTMS as an alternative or complementary treatment in case of disabling VH. Below, we discuss our results in more detail.

5.4.1 The key role of hippocampal formation in VH

When evaluating the functional brain connectivity network between SMA and the 'rich-club' regions after rTMS treatment, we found a robust increase in the functional centrality value and a distinct change in the connectivity pattern between the hippocampal formation and the SMA. In accordance with this result, previous studies have reported a key role of the hippocampus in Parkinson's disease with VH (Amad et al. 2014; Yao et al. 2016). Besides other functions, the hippocampus is crucial for integration of dorsal and ventral visual streams and is instrumental in complex visual processing, such as visual scene representation, image perception, visuospatial attention and memory (Braak et al. 1996; Hannula and Ranganath 2009; Chan et al. 2017). Consistent with these hypothetical roles of the hippocampus, disrupted integration between external visual stimuli and internal image perception can be expressed by decreased connectivity of the hippocampal area, as was seen in our pre-rTMS data, possibly contributing to the clinical severity of VH. The increased connectivity observed between the SMA and hippocampus after rTMS treatment correlates closely with the clinical improvement in existing VH of our patient. Even in the absence of a direct anatomical connection between SMA and hippocampal formation (Jürgens 1984), this suggests that rTMS stimulation can propagate and induce changes in cortical activity beyond the targeted area (Sale et al. 2015).

5.4.2 rTMS effects are selective to VH network areas

We found significant and selective differences in centrality values for specific brain areas between pre-rTMS and post-rTMS, e.g. the SMA, hippocampus and occipital pole. Of note, we found a difference in centrality in the occipital pole, an area involved in bottom-up visuo-perceptual processing (Thiebaut de Schotten et al. 2014). Like the hippocampal formation, this area is also known to be associated with VH (Lefebvre et al. 2016). This again suggests that rTMS treatment by targeting the SMA affects areas involved in VH.

We noted that a change in centrality was absent in the PCN (the control area). Although the PCN is part of the rich club network, it is associated with different neurocognitive processes including episodic memory, visuo-spatial information preprocessing and mental and motor imagery (Cavanna and Trimble 2006). Nonetheless, a strong functional connectivity between SMA and PCN is believed to be present in order to preprocess conscious visual-motor imagery stimuli (Malouin et al. 2003; Ogiso, Kobayashi, and Sugishita 2000). Combined, these results show that the effect of rTMS is not brain-wide, but rather specific.

5.4.3 VH and rTMS: addressing the challenge of personalized, non-invasive brain stimulation treatment

Several theories have been proposed about the mechanisms that may cause VH (Lewis et al. 2014; Shine et al. 2014, 2011, 2015; Collerton, Perry, and McKeith 2005). An interesting one is the global neural network (Lewis et al. 2014) approach. It is based on an imbalance and disrupted connectivity between well-known brain networks: the default mode network (DMN) (Greicius et al. 2003; Raichle et al. 2001; Raichle 2015) and the ventral and dorsal attentional networks (VAN and DAN, respectively) (Corbetta and Shulman 2011; Vossel, Geng, and Fink 2014). The observed imbalance between various brain networks might be due to one of two common factors found in subjects suffering from VH: (i) defects in visual bottom-up information processing (Meyer 2011), or (ii) an impairment of attentional systems (Dayan et al. 2013). In both cases, the location of the impairment is assumed to be strongly related to the nature of the VH (Anderson and Rizzo 1994). Another model, the perception and attention deficit (PAD) model of Collerton et al., aims to explain and integrate the multifactorial aspects that commonly characterize VH (Collerton, Perry, and McKeith 2005). Like the aforementioned theories, the PAD model hypothesizes that VH are caused by a combination of uncorrelated integration processes of the attentional and visual systems. Although the PAD model and the proposed common neural network theory can account for many aspects of VH, both models are incomplete, but they are possible contributors to the underlying pathogenesis.

Although no theory for VH (Diederich NJ, Goetz CG and Stebbins GT) has been generally accepted, it seems likely that various pathologies affecting different brain regions can trigger VH through different neuronal mechanisms. Conversely, different brain regions – if connected to one another – can strongly influence the same network activity. This supports our choice of SMA as a target region.

The fact that no unifying theory has been accepted to date indicates another important aspect of VH: that the phenotype of VH is subject-specific and disorder-related. This may underlie the variability in the success of rTMS treatments for VH thus far. A few prior case studies of VH treated with rTMS have been reported, all of which selected different target areas. In two of these cases, the subjects were suffering from Charles Bonnet syndrome; based on eyes-open fMRI data, different areas of the visual cortex were chosen as the target for rTMS treatment (Meppelink et al. 2010) In other case studies of VH patients with schizophrenia (Jolfaei, Naji, and Esfehani 2016), the occipito-temporal sulcus and the visual cortex were identified as target sites for rTMS treatment based on fMRI data. In our study, we identified a different target area for rTMS: the SMA. Besides the convenient anatomical location for rTMS treatment, the SMA plays a key role in motor imagery, a feature present in the majority of the VH experiences reported by our subject. Therefore, a customized therapy based on the ECM method as proposed here might result not only in more effective rTMS treatment, but also deeper insight into the mechanisms underlying VH.

5.4.4 Limitations and future work

In this study, we present a novel rTMS target selection approach based on ECM at the single subject level. Future studies may benefit by applying this general method to guide non-invasive brain stimulation for treatment of other neurological diseases. Moreover, the effect of different types and protocols of noninvasive brain stimulation can be monitored using the statistical approach proposed here.

We identified SMA as an effective rTMS target area for VH. Further research should be undertaken to investigate the possible role of SMA in VH, the functional network architecture underlying VH, and the directionality and causality therein.

A clear limitation of the current study is the lack of a sham/placebo condition in the same patient as it makes hard to objectively quantify the association between treatment and reduction of VH intensity. Such a trial was attempted but failed for several reasons. The patient had a severe off period just before the post-sham fMRI scanning which made it necessary for her to take extra L-dopa just before the scanning resulting in hyperkinesia. Therefore, these fMRI data could not be compared directly against the pre-sham data, thus preventing complete sham-control. Nonetheless, we

found repeatable functional connectivity patterns across baseline, pre-treatment and pre-sham scans (Supplementary Material, S1 and Table S1). This suggests that the hubs resulting from the ECM mapping are stable over time.

Repeating the fMRI sessions once more was considered too demanding for the patient. However, we decided to repeat the rTMS treatment after 15 months but with only 30 Hz theta burst stimulation during 10 days applied to the target region identified in our ECM analysis (Figure 1, Panel C). The patient again reported a clear reduction in VH intensity of approximately 35%, starting with a mean VH intensity of NRS 9, which was reduced to NRS 6 after 10 days. Also, this time the VH-ds showed the largest reduction. This finding suggests that an individually identified target hub may be stable over time, which makes rs-fMRI based ECM a clinically viable method.

5.5 CONCLUSION

Applying ECM to rs-fMRI based data enabled us to identify a viable target area for the rTMS treatment at the single patient level. Moreover, changes in the ECM values were used to establish the selective effect of this noninvasive brain stimulation. We conclude that our treatment was successful, based on the reported decrease in VH intensity post-treatment and the selective change in ECM values of the identified target area (SMA). Moreover, the change in functional connectivity of the SMA to the hippocampal area indicates a potential functional explanation for the decrease in VH. Hence, effective rTMS stimulation probably requires either inducing neuroplastic changes in the appropriate area directly or in areas functionally connected to it. This potentially expands the options for using rTMS as treatment, and also indicates the complexity of the mechanisms underlying VH.

REFERENCES

Amad, A., A. Cachia, P. Gorwood, D. Pins, C. Delmaire, B. Rolland, M. Mondino, P. Thomas, and R. Jardri. 2014. "The Multimodal Connectivity of the Hippocampal Complex in Auditory and Visual Hallucinations." *Molecular Psychiatry* 19 (2): 184–91.

Anderson, S. W., and M. Rizzo. 1994. "Hallucinations Following Occipital Lobe Damage: The Pathological Activation of Visual Representations." *Journal of Clinical and Experimental Neuropsychology* 16 (5). https://doi.org/10.1080/01688639408402678.

Braak, Heiko, Eva Braak, Deniz Yilmazer, and Jurgen Bohl. 1996. "Topical Review: Functional Anatomy of Human Hippocampal Formation and Related Structures." *Journal of Child Neurology*. https://doi.org/10.1177/088307389601100402.

Bright, Molly G., and Kevin Murphy. 2015. "Is fMRI 'noise' Really Noise? Resting State Nuisance Regressors Remove Variance with Network Structure." *NeuroImage*. https://doi.org/10.1016/j.neuroimage.2015.03.070.

Cavanna, Andrea E., and Michael R. Trimble. 2006. "The Precuneus: A Review of Its Functional Anatomy and Behavioural Correlates." *Brain: A Journal of Neurology* 129 (Pt 3): 564–83.

Chan, Russell W., Alex T. L. Leong, Leon C. Ho, Patrick P. Gao, Eddie C. Wong, Celia M. Dong, Xunda Wang, et al. 2017. "Low-Frequency Hippocampal-Cortical Activity Drives Brain-Wide Resting-State Functional MRI Connectivity." *Proceedings of the National Academy of Sciences of the United States of America* 114 (33): E6972–81.

Collerton, D., E. Perry, and I. McKeith. 2005. "Why People See Things That Are Not There: A Novel Perception and Attention Deficit Model for Recurrent Complex Visual Hallucinations." *The Behavioral and Brain Sciences* 28 (6). https://doi.org/10.1017/S0140525X05000130.

Corbetta, M., and G. L. Shulman. 2011. "Spatial Neglect and Attention Networks." *Annual Review of Neuroscience* 34. https://doi.org/10.1146/annurev-neuro-061010-113731.

Dayan, Eran, Nitzan Censor, Ethan R. Buch, Marco Sandrini, and Leonardo G. Cohen. 2013. "Noninvasive Brain Stimulation: From Physiology to Network Dynamics and Back." *Nature Neuroscience*. https://doi.org/10.1038/nn.3422.

Fox, Michael D., Randy L. Buckner, Hesheng Liu, M. Mallar Chakravarty, Andres M. Lozano, and Alvaro Pascual-Leone. 2014. "Resting-State Networks Link Invasive and Noninvasive Brain Stimulation across Diverse Psychiatric and Neurological Diseases." *Proceedings of the National Academy of Sciences of the United States of America* 111 (41): E4367–75.

Fregni, Felipe, and Alvaro Pascual-Leone. 2007. "Technology Insight: Noninvasive Brain Stimulation in Neurology—perspectives on the Therapeutic Potential of rTMS and tDCS." *Nature Clinical Practice Neurology*. https://doi.org/10.1038/ncpneuro0530.

Greicius, B. Krasnow, A. L. Reiss, and V. Menon. 2003. "Functional Connectivity in the Resting Brain: A Network Analysis of the Default Mode Hypothesis." *Proceedings of the National Academy of Sciences of the United States of America* 100 (1). https://doi.org/10.1073/pnas.0135058100.

Hallett, Mark. 2007. "Transcranial Magnetic Stimulation: A Primer." *Neuron*. https://doi.org/10.1016/j.neuron.2007.06.026.

Hannula, Deborah E., and Charan Ranganath. 2009. "The Eyes Have It: Hippocampal Activity Predicts Expression of Memory in Eye Movements." *Neuron* 63 (5): 592–99.

Hartong, Dyonne T., Eliot L. Berson, and Thaddeus P. Dryja. 2006. "Retinitis Pigmentosa." *The Lancet*. https://doi.org/10.1016/s0140-6736(06)69740-7.

Heuvel, M. P. van den, and O. Sporns. 2011. "Rich-Club Organization of the Human Connectome." *The Journal of Neuroscience: The Official Journal of the Society for Neuroscience* 31 (44). https://doi.org/10.1523/JNEUROSCI.3539-11.2011.

Hoffman, R. E., M. Hampson, K. Wu, A. W. Anderson, J. C. Gore, R. J. Buchanan, R. T. Constable, K. A. Hawkins, N. Sahay, and J. H. Krystal. 2007. "Probing the Pathophysiology of Auditory/Verbal Hallucinations by Combining Functional Magnetic Resonance Imaging and Transcranial Magnetic Stimulation." *Cerebral Cortex*. https://doi.org/10.1093/cercor/bhl183.

Jardri, Renaud, Delphine Pins, Maxime Bubrovszky, Bernard Lucas, Vianney Lethuc, Christine Delmaire, Vincent Vantyghem, Pascal Despretz, and Pierre Thomas. 2009. "Neural Functional Organization of Hallucinations in Schizophrenia: Multisensory Dissolution of Pathological Emergence in Consciousness." *Consciousness and Cognition*. https://doi.org/10.1016/j.concog.2008.12.009.

Jolfaei, Atefeh Ghanbari, Borzooyeh Naji, and Mehdi Nasr Esfehani. 2016. "Repetitive Transcranial Magnetic Stimulation Magnetic Stimulation in Resistant Visual Hallucinations in a Woman With Schizophrenia: A Case Report." *Iranian Journal of Psychiatry and Behavioral Sciences*. https://doi.org/10.17795/ijpbs-3561.

Jürgens, U. 1984. "The Efferent and Afferent Connections of the Supplementary Motor Area." *Brain Research*. https://doi.org/10.1016/0006-8993(84)91341-6.

Labriffe, Matthieu, Cédric Annweiler, Liubov E. Amirova, Guillemette Gauquelin-Koch, Aram Ter Minassian, Louis-Marie Leiber, Olivier Beauchet, Marc-Antoine Custaud, and Mickaël Dinomais. 2017. "Brain Activity during Mental Imagery of Gait Versus Gait-Like Plantar Stimulation: A Novel Combined Functional MRI Paradigm to Better Understand Cerebral Gait Control." *Frontiers in Human Neuroscience* 11 (March): 106.

Lefebvre, Stéphanie, Guillaume Baille, Renaud Jardri, Lucie Plomhause, Sébastien Szaffarczyk, Luc Defebvre, Pierre Thomas, Christine Delmaire, Delphine Pins, and Kathy Dujardin. 2016. "Hallucinations and Conscious Access to Visual Inputs in Parkinson's Disease." *Scientific Reports*. https://doi.org/10.1038/srep36284.

Lewis, Simon J. G., James M. Shine, Daniel Brooks, and Glenda M. Halliday. 2014. "Hallucinogenic Mechanisms: Pathological and Pharmacological Insights." *The Neuroscience of Visual Hallucinations*. https://doi.org/10.1002/9781118892794.ch6.

Lima, César F., Saloni Krishnan, and Sophie K. Scott. 2016. "Roles of Supplementary Motor Areas in Auditory Processing and Auditory Imagery." *Trends in Neurosciences* 39 (8): 527–42.

Malouin, Francine, Carol L. Richards, Philip L. Jackson, Francine Dumas, and Julien Doyon. 2003. "Brain Activations during Motor Imagery of Locomotor-Related Tasks: A PET Study." *Human Brain Mapping* 19 (1): 47–62.

Manford, M. 1998. "Complex Visual Hallucinations. Clinical and Neurobiological Insights." *Brain*. https://doi.org/10.1093/brain/121.10.1819.

Meppelink, A. M., B. M. de Jong, J. H. van der Hoeven, and T. van Laar. 2010. "Lasting Visual Hallucinations in Visual Deprivation; fMRI Correlates and the Influence of rTMS." *Journal of Neurology, Neurosurgery & Psychiatry*. https://doi.org/10.1136/jnnp.2009.183087.

Meyer, K. 2011. "Primary Sensory Cortices, Top-down Projections and Conscious Experience." *Progress in Neurobiology* 94 (4). https://doi.org/10.1016/j.

pneurobio.2011.05.010.

Monti, Martin M. 2011. "Statistical Analysis of fMRI Time-Series: A Critical Review of the GLM Approach." *Frontiers in Human Neuroscience* 5 (March): 28.

Ogiso, T., K. Kobayashi, and M. Sugishita. 2000. "The Precuneus in Motor Imagery: A Magnetoencephalographic Study." *Neuroreport* 11 (6): 1345–49.

Raichle, M. E. 2015. "The Restless Brain: How Intrinsic Activity Organizes Brain Function." *Philosophical Transactions of the Royal Society of London. Series B, Biological Sciences* 370 (1668). https://doi.org/10.1098/rstb.2014.0172.

Raichle, M. E., A. M. MacLeod, A. Z. Snyder, W. J. Powers, D. A. Gusnard, and G. L. Shulman. 2001. "A Default Mode of Brain Function." *Proceedings of the National Academy of Sciences of the United States of America* 98 (2). https://doi.org/10.1073/pnas.98.2.676.

Räth, C., and R. Monetti. 2009. "Surrogates with Random Fourier Phases." *Topics on Chaotic Systems*. https://doi.org/10.1142/9789814271349_0031.

Sale, Martin V., Jason B. Mattingley, Andrew Zalesky, and Luca Cocchi. 2015. "Imaging Human Brain Networks to Improve the Clinical Efficacy of Non-Invasive Brain Stimulation." *Neuroscience & Biobehavioral Reviews*. https://doi.org/10.1016/j.neubiorev.2015.09.010.

Schreiber, Thomas, and Andreas Schmitz. 1996. "Improved Surrogate Data for Nonlinearity Tests." *Physical Review Letters*. https://doi.org/10.1103/physrevlett.77.635.

Shine, J. M., G. M. Halliday, S. L. Naismith, and S. J. Lewis. 2011. "Visual Misperceptions and Hallucinations in Parkinson's Disease: Dysfunction of Attentional Control Networks?" *Movement Disorders: Official Journal of the Movement Disorder Society* 26 (12). https://doi.org/10.1002/mds.23896.

Shine, J. M., R. Keogh, C. O'Callaghan, A. J. Muller, S. J. Lewis, and J. Pearson. 2015. "Imagine That: Elevated Sensory Strength of Mental Imagery in Individuals with Parkinson's Disease and Visual Hallucinations." *Proceedings. Biological Sciences / The Royal Society* 282 (1798). https://doi.org/10.1098/rspb.2014.2047.

Shine, J. M., C. O'Callaghan, G. M. Halliday, and S. J. Lewis. 2014. "Tricks of the Mind: Visual Hallucinations as Disorders of Attention." *Progress in Neurobiology* 116 (May). https://doi.org/10.1016/j.pneurobio.2014.01.004.

Singh, Aditya, Tracy Erwin-Grabner, Grant Sutcliffe, Andrea Antal, Walter Paulus, and Roberto Goya-Maldonado. n.d. "Resting State fMRI Based Target Selection for Personalized rTMS: Stimulation over the Left DLPFC Temporarily Alters the Default Mode Network in Healthy Subjects." https://doi.org/10.1101/344390.

Sporns, Olaf, Christopher J. Honey, and Rolf Kötter. 2007. "Identification and Classification of Hubs in Brain Networks." *PloS One* 2 (10): e1049.

Thiebaut de Schotten, Michel, Marika Urbanski, Romain Valabregue, Dimitri J. Bayle, and Emmanuelle Volle. 2014. "Subdivision of the Occipital Lobes: An Anatomical and Functional MRI Connectivity Study." *Cortex; a Journal Devoted to the Study of the Nervous System and Behavior* 56 (July): 121–37.

Vossel, S., J. J. Geng, and G. R. Fink. 2014. "Dorsal and Ventral Attention Systems: Distinct Neural Circuits but Collaborative Roles." *The Neuroscientist: A Review Journal Bringing Neurobiology, Neurology and Psychiatry* 20 (2). https://doi.org/10.1177/1073858413494269.

Waters, Flavie, Daniel Collerton, Dominic H. Ffytche, Renaud Jardri, Delphine Pins, Robert Dudley, Jan Dirk Blom, et al. 2014. "Visual Hallucinations in the Psychosis Spectrum and Comparative Information From Neurodegenerative Disorders

and Eye Disease." *Schizophrenia Bulletin*. https://doi.org/10.1093/schbul/sbu036.

"Website." n.d. Accessed April 29, 2021. Diederich NJ, Goetz CG and Stebbins GT. The pathology of hallucinations: one or several points of processing breakdown? The Neuroscience of Visual Hallucinations 281–306 (Wiley- Blackwell, 2014). https://doi.org/10.1002/9781118892794.ch12.

Wink, Alle Meije, Jan C. de Munck, Ysbrand D. van der Werf, Odile A. van den Heuvel, and Frederik Barkhof. 2012. "Fast Eigenvector Centrality Mapping of Voxel-Wise Connectivity in Functional Magnetic Resonance Imaging: Implementation, Validation, and Interpretation." *Brain Connectivity*. https://doi.org/10.1089/brain.2012.0087.

Yao, Nailin, Charlton Cheung, Shirley Pang, Richard Shek-kwan Chang, Kui Kai Lau, John Suckling, Kevin Yu, et al. 2016. "Multimodal MRI of the Hippocampus in Parkinson's Disease with Visual Hallucinations." *Brain Structure & Function* 221 (1): 287–300.